Cadence Simulation Environment for Contactless Near-Field Communication tags

R. Stadlmair and M. Gebhart
NXP Semiconductors Austria GmbH, Gratkorn, Austria
rainer.stadlmair@nxp.com, gebhart@ieee.org

***Abstract* — this paper introduces a model to verify the contactless performance of a transponder front end using a Cadence based simulation environment. The air interface between reader and transponder is thoroughly described and important values and equations are presented. They build the basics for an equivalent electrical model that can be used for simulations using spice simulators. This model is incorporated into the simulation environment and simulated together with a transponder front end designed in a 140 nm CMOS process. The paper gives a rough insight into the functionality of a transponder front end, describes certain scenarios, critical with regards to power consumption, and shows simulation results using the described model.**

I. INTRODUCTION

It is *interoperability* of products and technologies of manufacturers for contactless communication in the near field which brings the promised advantages to the individual consumer. This requires product conformance to the base standards, preferably to such standards, which are already proven and have been developed over years, supporting billions of devices in the field. Examples are the successful standards for contactless Smartcards, like ISO/IEC14443 for secure personal proximity cards, or ISO/IEC15693 for vicinity tags which is also implemented for Item Level Tagging (ILT) in ISO/IEC18000-3 for tags and labels in logistics applications, or the booming Near Field Communication (NFC) ISO/IEC18092, consisting of the protocol of ISO/IEC14443A at base data rate, and the japanese FeliCa protocol for higher data rates.

To account for world-wide interoperability, the standardization of these Information Technologies (IT) is done in international working groups according to the rules of the International Organization for Standardization (ISO) and the International Electrotechnical Commission (IEC), which build the joint technical committee 1 (JTC1) for this purpose. Although standards are a result of political compromises and individual experts may know more appropriate solutions, new technical developments are a welcome basis to these committees, such as conference contributions which have been peer-reviewed and so reflect the opinion of several experts.

The concept of these proximity base standards is separated in layers, i.e. for ISO/IEC14443 these cover specifications for geometry and physical properties [1], for the radio signal air interface [2], for data formats and anticollision mechanism [3] and for transmission protocol, security and enhanced functions in [4]. Specific test equipment and test methods are described in a test standard, i.e. ISO/IEC10373-6, to verify standard conformance at the air interface. This test equipment is also used by accredited test labs e.g. to certify compliance for electronic passports, which is a prominent application for such devices. However, the test standard just specifies an antenna arrangement, the choice of appropriate measurement instruments to generate and analyse signals is up to the test lab.

From this perspective it makes sense to integrate this antenna arrangement testbench also in the development environment for integrated circuits, which are intended for contactless applications. Signal transitions like current peaks caused by state switches are usually simulated with Spice or other analogue simulators using Electronic Design Automation (EDA) tools from Cadence or other vendors.

II. AIR INTERFACE TEST BENCH IN CADENCE ENVIRONMENT

A. Setup components

The coaxial antenna arrangement for card test [5] emulates the physical layer properties of a reader at the air interface. Some properties and reasoning for these specifications can be found in [16]. The arrangement shown in fig. 1 consists of the following components:

a) The *proximity coupling device* (PCD) antenna, shown in fig. 2. This is a 1 turn (electrically compensated) circular loop antenna placed in center of the arrangement, to emit the *H*-field.

b) The *calibration coil* on one side of the PCD antenna, shown in fig. 3. This is a rectangular shape one-turn loop coil intended to measure the (perpendicular) *H*-field at carrier frequency averaged over antenna area.

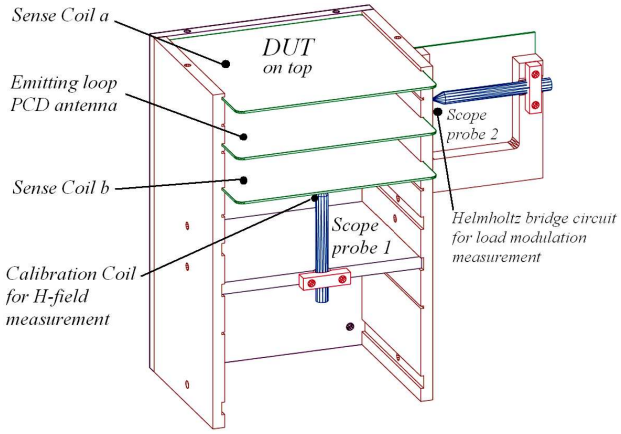

Figure 1. Fixture for the coaxial ISO/IEC10373-6 antenna arrangement.

c) The *device under test* (DUT) on the other side of the PCD antenna. This is a contactless transponder, which means e.g. a testboard antenna including a variable capacitor for resonance frequency adjustment and a chip engineering sample.

d) Two symmetrical *sense coils* on left and right side of the PCD antenna, shown in fig. 4. These are rectangular shaped one-turn loop coils connected over an adjustable resistor bridge. The intention is to compensate induced voltage of the primary field of the PCD antenna and to measure the secondary field emitted by the DUT, i.e. *load modulation* at two *sideband frequencies*.

Different to a real reader environment the constant distances of all coils in the coaxial arrangement are well defined and carefully chosen e.g. to have a homogenous *H*-field strength in DUT antenna plane over the card antenna area. This allows to specify fixed coupling factors and equivalent circuit parameters for the arrangement in the Cadence simulation environment.

The test standard specifies the layout of the coils in the coaxial antenna arrangement, and some component values, e.g. for the impedance matching network of the PCD antenna. [16] describes measurement methods to extract equivalent circuit element values for the individual coils, e.g. for a simple parallel equivalent circuit, valid at the carrier frequency f_C = 13.56 MHz.

TABLE I. PCD 1 ANTENNA ARRANGEMENT [5], PCD 2 ANTENNA ARRANGEMENT [8] GEOMETRY AND EXTRACTED EQUIVALENT CIRCUIT

		PCD 1 (for class 1 – 3)			***PCD 2 (for class 4 – 6)***		
		PCD	SenseCoil	CalCoil	PCD	SenseCoil	CalCoil
r	mm	75	---	---	50	---	---
l x w	mm	---	100 x 70	72 x 42	---	60 x 47	46 x 24
L_A	µH	0.480	0.422	0.204	0.324	0.315	0.170
C_A	pF	26.06	5.26	9.00	18.40	3.93	8.00
R_A	Ω	7057	5653	1766	1520	2185	1104

B. Matching network calculation

Due to fabrication and component tolerances there may still be small deviations e.g. between fabricated PCD antenna printboards. Thus for practical work in the lab, the correct 50 Ω antenna matching is always verified by measurement (e.g. using a network analyzer) after assembly of the components in order to compensate for antenna measurement deviations and component tolerances. As these aspects can be exclued in the Cadence simulation environment, the appropriate choice here is to use the exact calculated values. The best approach is to calculate the exact element values for the matching network, based on the antenna equivalent circuit, analytically. The detailed derivation is described in [17].

The impedance Z_{LOAD} of the equivalent circuit in fig. 1 at the driver amplifier connection can be described by

$$Z_{LOAD} = \frac{sR_A L_A}{s^2 R_A L_A (C_A + C_P) + sL_A + R_A} + \frac{1}{sC_S}. \quad (1)$$

Resolving for serial and parallel capacitance of the matching network results a quadratic equation. The two solutions for the parallel capacitor are given by

$$C_{P\,a,b} = -\frac{p}{2} \pm \sqrt{\frac{p^2}{4} - q} \quad (2)$$

where $p = \frac{2\omega^2 L_A C_A - 2}{\omega^2 L_A}$ (3)

and

$$q = \frac{R_D R_A \left(\omega^4 R_A {L_A}^2 {C_A}^2 - 2\omega^2 R_A L_A C_A + 1\right) - \omega^2 (R_A - R_D)}{\omega^4 R_D {R_A}^2 {L_A}^2} \quad (4)$$

Only positive solutions do have a phyiscal representation by a capacitor. Once C_P is determined, also C_S can be calculated, using one of the two equations (5, 6)

$$C_{S,a} = \frac{L_A}{R_D R_A - \omega^2 R_D R_A L_A (C_A + C_P)} \quad (5)$$

$$C_{S,b} = \frac{-\omega^2 R_A L_A (C_A + C_P) + R_A}{\omega^2 L_A (R_A - R_D)}. \quad (6)$$

In general it is not possible to match all loads using this "L"- topology for the matching network, but typical antennas in the HF RFID context are covered, and by choosing capacitors of the right dielectric material (e.g. C0G), losses in the network are negligible. Thus component values of table 2 are here slightly different to the standard component list.

Due to time constants, the test standard specifies two different *Q*-factors and matching networks for the layout of the larger PCD1 antenna [5], and one for the layout of the smaller PCD2 antenna [8].

In detail it is important to differentiate the *antenna Q-factor* Q_A (for an open antenna connection), which is defined by the relation of *reactive* and *active impedance*,

$$Q_A = \frac{\omega L_A}{R_{SERIAL}} = \frac{R_{PARALLEL}}{\omega L_A} \quad (7)$$

and the *operational Q-factor* for the antenna terminated by the 50 Ohm impedance of the amplifier. The *operational Q-factor* is half the value of the antenna Q-factor (due to 50 Ω load matching), and determines the time and amplitude values [18], specified by the standard [2]. The antenna Q-factor is about 35 for the PCD1 antenna which can be used to measure the base data rate (BDR) of ~ 106 kbit/s, it is about 8.3 for the PCD1 antenna which can be used to measure also higher data rates (HDR) of 212, 424 and 848 kbit/s, and it is about 8.6 for the PCD2 antenna which can be used to measure BDR and HDR for small transponder antenna size classes.

TABLE II. MATCHING NETWORK COMPONENTS FOR PCD1 BDR AND HDR ANTENNA, AND PCD2 HDR ANTENNA

Component	***Unit***	***PCD1 BDR***	***PCD1 HDR***	***PCD2 HDR***
R_E	Ω	0.94	4.7	2.7
C_S	pF	49.2	104	121
C_P	pF	226	186	311

Note: Exact calculated values for antenna parameters acc. table 1, including trimm cap. values.

C. Coupling factors of arrangement

To take into account the geometry of the coaxial loop antenna arrangement, we have to consider coupling. The coupling factor can be calculated from conductor geometry and causes mutual inductance, changing the effective electrical parameters of all coils and allowing signals to couple from one to other coils.

Values for coupling factors in the antenna arrangement 1 and 2 are given in table 3.

TABLE III. COUPLING FACTORS FOR THE COAXIAL ANTENNA ARRANGEMENTS

	***k* PCD 1 arrangement**	***k* PCD 2 arrangement**
L_{DUT} - L_{SENSEA}	0.197*	0.167**
L_{PCD} - L_{DUT}	0.063*	0.058**
L_{SENSEA} - L_{SENSEB}	0.024	0.022
L_{PCD} - L_{SENSEA}	0.089	0.081
L_{PCD} - L_{SENSEB}	0.089	0.081
L_{PCD} - $L_{CALCOIL}$	0.056	0.042
L_{SENSEB} - $L_{CALCOIL}$	0.017	0.014

* Class 1 antenna 74 x 45 mm, ** class 4 antenna 48 x 25 mm

D. Verification of the H-field strength

Most characterization measurementes are performed over an *H*-field range (H_{MIN} ... H_{MAX}) which is specified for each transponder antenna class in the base standard. Actual values are shown in table IV. It is important to verify the correct *H*-field strength also for the simulation environment. *H*-field is measured as voltage induced in the Calibration Coil, with the DUT in the antenna arrangement. The alternating *H*-field amplitude is measured at the carrier frequency f_C = 13.56 MHz while no data is transmitted, which means that also a narrow-band equivalent circuit representation (e.g. parallel resonant circuits) will deliver accurate results.

For a homogenous *H*-field strength over the area of the Calibration Coil, the induced voltage $U_{I,RMS}$ is given by

$$U_{I,RMS} = 2\pi\ f_C \cdot \mu_0 \cdot A \cdot H_{RMS} \tag{13}$$

where *A* is the Calibration Coil antenna area of ~ 3000 mm² for the Calibration Coil 1. This means about 0.32 V(rms) per A/m(rms). For the Calibration Coil 2 the area is about 1100 mm², this means about 0.118 V per A/m.

The emitted *H*-field strength over distance close to the antenna conductor can be calculated e.g. by the extended Biot-Savart equation [16]. For the PCD1 arrangement, a total (*active* and *reactive*) current of 1 Ampere (rms) in the antenna conductor results at f_C in an *H*-field strength of about 4.77 A/m(rms) at the specified distance of 37.5 mm to the emitting PCD1 loop antenna. Any loading due to proximity coupling of DUT to PCD antenna will reduce the emitted *H*-field but will also reduce the PCD antenna current – current and *H*-field are directly related. This so-called loading effect, which is non-linear over varied *H*-field strength due to a voltage limiter on the Smartcard chip, can be compensated also in simulation. For the PCD 2 arrangement, a total current in the 1-turn antenna of 1 A results at f_C in an *H*-field strength of 7.5 A/m at the specified distance of 23.0 mm for the planes of DUT and Calibration Coil 2 to the emitting PCD2 loop antenna.

The voltage at the amplifier output (which due to 50 **Ω** load matching is half the voltage of the driver voltage source U_D in simulation) is given by

$$U_{V\_ANT} = \sqrt{\frac{I_A^{\,2} \cdot 2\pi\ f_C \cdot L_A}{N^2 \cdot Q_A} \cdot R_D}\ . \tag{14}$$

Without any DUT in the ISO/IEC10373-6 test setup, 1 Ampere in the antenna conductor for the PCD1 BDR antenna with antenna Q-factor of about 35 means 7.67 V(rms) at the amplifier output, for the PCD1 HDR antenna with antenna Q-factor of about 8.3 this means 15.71 V(rms) at the amplifier output, and for the PCD2 HDR antenna with antenna Q-factor of about 8.6 this means 12.65 V(rms) at the amplifier output. For this calculation step, we have neglected any DUT loading.

E. Simulation Model

The simulation model for the ISO/IEC10373-6 antenna arrangement, in brief ISO model, is built of ideal network elements which have constant values assigned so that it can be simulated independently of any process variations. Process model files used for simulation of CMOS process variations are not applied for the simulation of the ISO model. Additionally the values for the inductance, parallel resistance and capacitance of the transponder antenna can be parameterized in order to use the model independently of the antenna class. Values will be assigned during simulating using the Virtuoso® Analog Design Environment (ADE). The schematic is shown in fig. 5.

III. CONTACTLESS SMARTCARD CHIP FRONTEND

Contactless Smartcard chips compliant to the ISO/IEC14443 base standard [1-4] are operated in a resonance circuit. In order to achieve an optimum contactless power transfer from reader to transponder card and good operating distance, the resonance frequencies of reader and card will be tuned close to the carrier frequency f_C = 13.56 MHz of the system. However, depending on intended applications and operating conditions (e.g. multiple Card operation, transponder antenna size and manufacturing tolerances of chip and antenna) the transponder resonance circuit can be tuned to a higher resonance frequency by intention, to ensure the optimum performance.

A. Functional analogue blocks overview

A contactless transponder analogue front end usually consists of various functional blocks, such as the integrated resonance capacitor, a rectifier, voltage regulators and limiters, demodulator and load modulator and various sensors as part of the security system, which shall provide a stable supply voltage and proper means of communication for the digital processing unit. In this paper we focus on the simulation of the resonance circuit using Spice simulators in a Cadence EDA environment. The remaining blocks will just be described briefly to give a rough overview on how a contactless transponder frontend works in general.

The damped resonance circuit consists of inductance, capacitance and resistance. Inductance is defined by the loop antenna coil, to which the chip is assembled and connected when the transponder is laminated into a card. Capacitance is provided by an integrated capacitor that can withstand the high voltage levels which appear in the antenna resonance circuit, usually exceeding all other voltage levels in the chip. Resistance mainly is defined by the current consumption of the chip.

This resonance circuit is directly connected to a rectifier to generate a direct current (DC) voltage out of the induced sinewave voltage at carrier frequency.

A limiter is necessary to sink all current in excess provided by the antenna at high *H*-field conditions, to limit the chip internal voltage to a level, lower than the maximum voltage according process specifications, to prevent transistor gate oxide stress.

Depending on the complexity of the front end, regulators and DC/DC converters can be used to get several different supply voltage levels or power domains inside the device. Due to process requirements, state of the art contactless Smartcard chips also limit the coil voltage

to a defined level for operation, once the required minimum current is provided by the antenna circuit.

To extract transmitted command data out of the reader to card communication direction, a demodulator is used. For ISO/IEC14443A operation it generates digital pulses out of the analogue modulated carrier envelope, and a decoder then provides a digital bit stream out of the digital (modified Miller) channel coding by counting carrier cycles. This point is an interface between analogue and digital part of the chip.

For the communication direction of card to reader, the Smartcard chip can (more or less) short the antenna connection pins and in this way modulates the quality factor of the transponder resonance circuit. In proximity coupling to the reader antenna, this means an external modulation, changing the loading conditions to the reader antenna circuit dynamically (modulated by channel coding), the so-called *load modulation* (LM). Fig. 6 shows a simplified analogue front end for a contactless Smartcard transponder chip.

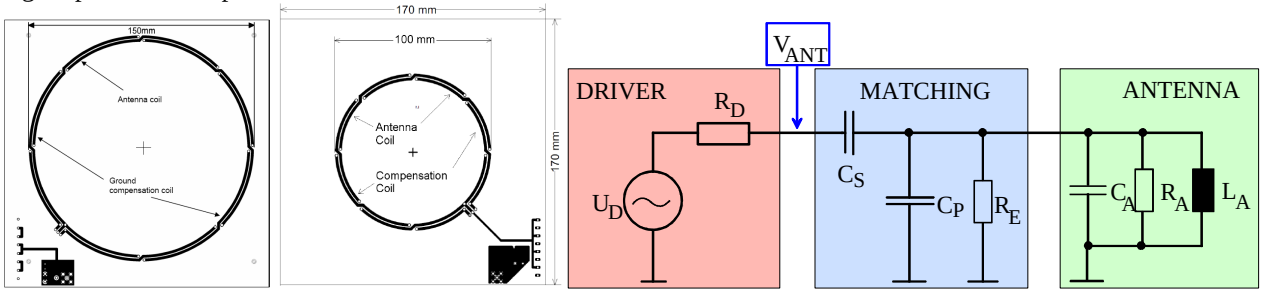

Figure 2. PCD1 antenna layout [5], PCD2 antenna layout [8], equivalent circuit including matching network and amplifier.

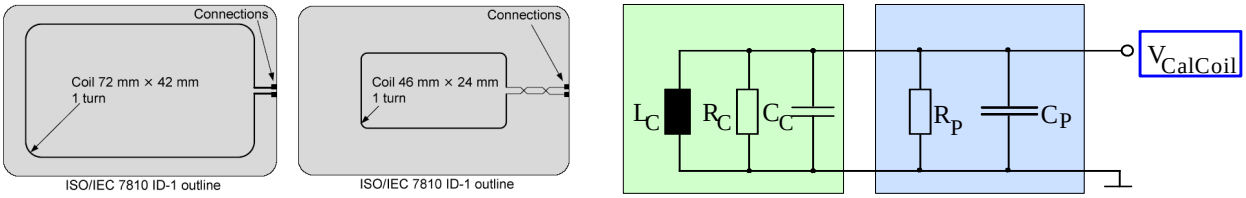

Figure 3. Calibration coil 1 layout [5], calibration coil 2 layout [8], equivalent circuit including scope probe.

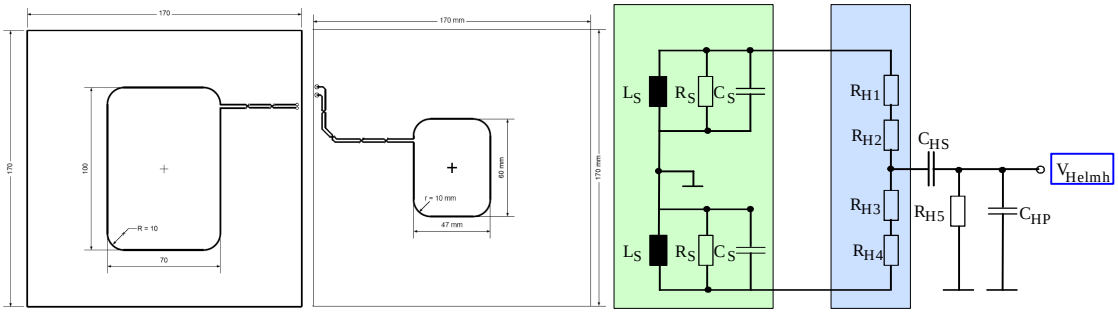

Figure 4. Sense coils 1 layout [5], sense coils 2 layout [8], equivalent circuit including *Helmholtz bridge* components and scope probe.

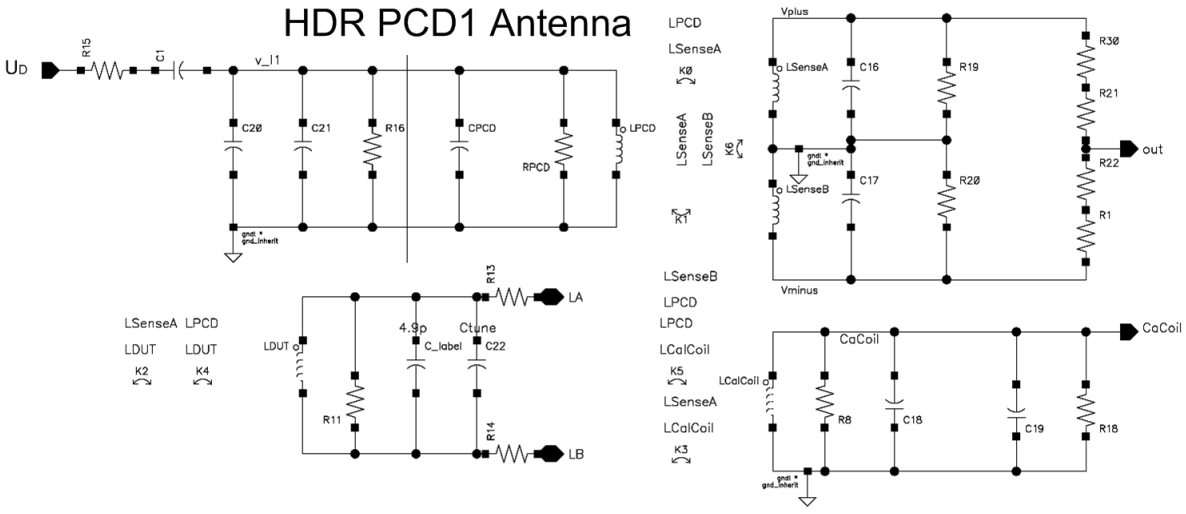

Figure 5. Complete ISO/IEC10373-6 Contactless Card test setup implemented in Cadence simulation environment for chip design.

TABLE IV. PROXIMITY ANTENNA GEOMETRY CLASSES AND SOME RELATED AIR INTERFACE PARAMETERS [1-8].

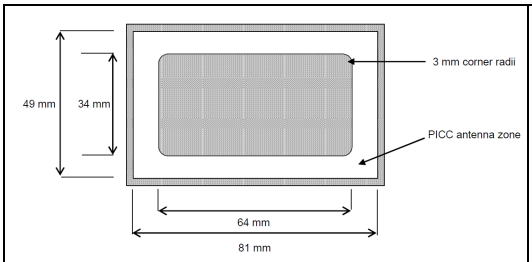

Parameter	*Value*	*Unit*
Transponder antenna class	1	---
PCD arrangement	1	---
H_{MIN}	1.5	A/m(rms)
H_{MAX}	7.5	A/m(rms)
Survival *H*-field	10 (average), 12 (peak)	
Min. load modulation	$22/H^{0.5}$	mV(p)

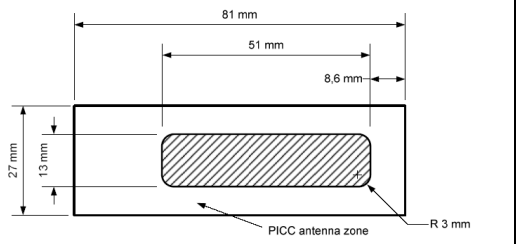

Parameter	*Value*	*Unit*
Transponder antenna class	2	---
PCD arrangement	1	---
H_{MIN}	1.5	A/m(rms)
H_{MAX}	8.5	A/m(rms)
Survival *H*-field	11.3 (average), 13.6 (peak)	A/m(rms)
min. load modulation	$22/H^{0.5}$	mV(p)

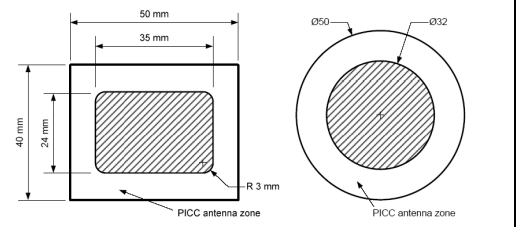

Parameter	*Value*	*Unit*
Transponder antenna class	3	---
PCD arrangement	1	---
H_{MIN}	1.5	A/m(rms)
H_{MAX}	8.5	A/m(rms)
Survival *H*-field	11.3 (average), 13.6 (peak)	A/m(rms)
min. load modulation	$22/H^{0.5}$	mV(p)

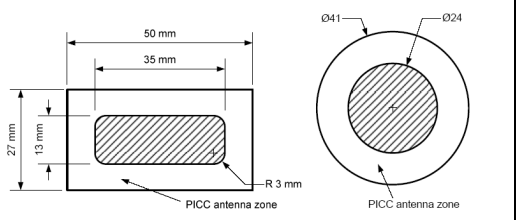

Parameter	*Value*	*Unit*
Transponder antenna class	4	---
PCD arrangement	2	---
H_{MIN}	2.0	A/m(rms)
H_{MAX}	12	A/m(rms)
Survival *H*-field	16 (average), 19.2 (peak)	A/m(rms)
min. load modulation	min. 18, $44/H^{0.5}$	mV(p)

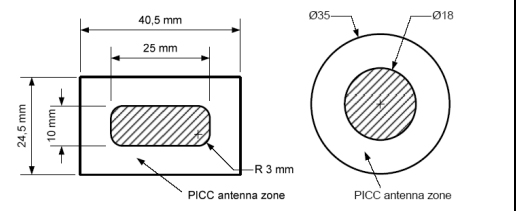

Parameter	*Value*	*Unit*
Transponder antenna class	5	---
PCD arrangement	2	---
H_{MIN}	2.5	A/m(rms)
H_{MAX}	14	A/m(rms)
Survival *H*-field	18.7 (average), 22.4 (peak)	A/m(rms)
min. load modulation	min. 18, $44/H^{0.5}$	mV(p)

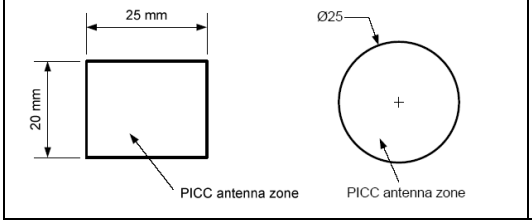

Parameter	*Value*	*Unit*
Transponder antenna class	6	---
PCD arrangement	2	---
H_{MIN}	4.5	A/m(rms)
H_{MAX}	18	A/m(rms)
Survival *H*-field	24 (average), 28.8 (peak)	A/m(rms)
min. load modulation	8	mV(p)

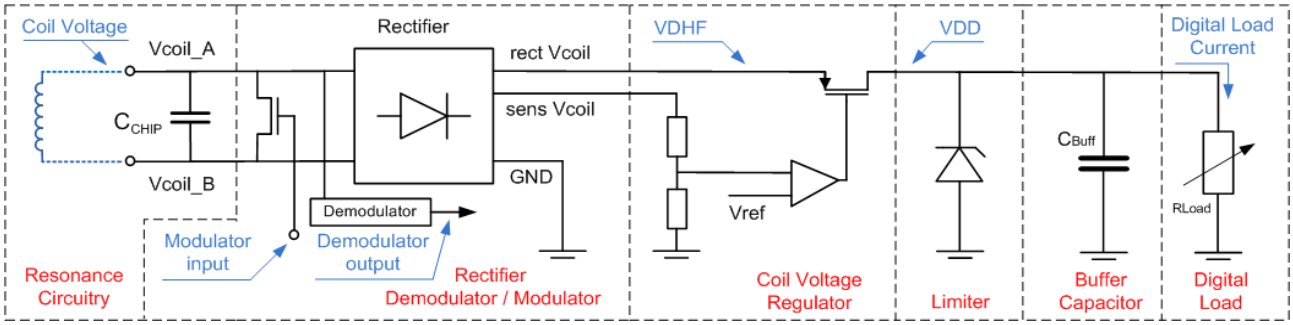

Figure 6. Contactless Proximity Smartcard transponder chip analog front end.

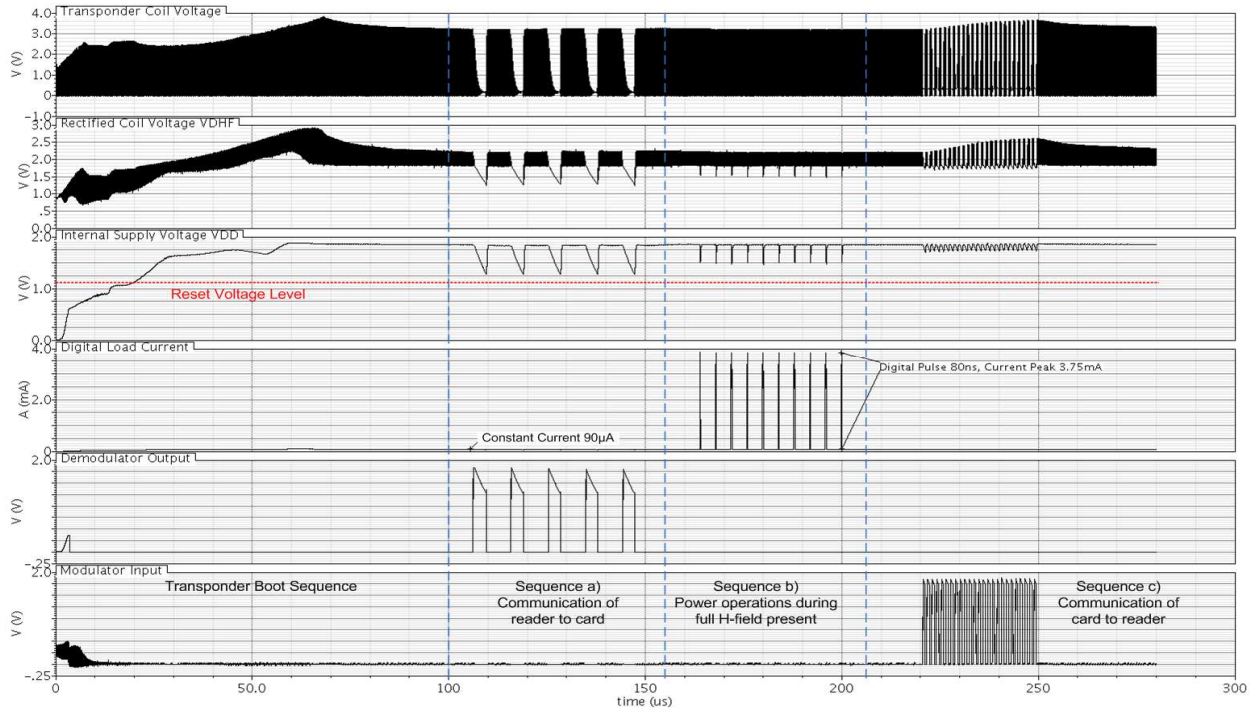

Figure 7. Reference transaction sequence simulated in Cadence at 13.56MHz and *H*-field strength of around 500mA/m.

B. Reset triggers

In order to be operable and sustain the supply voltage level during communication a buffer capacitor is used. It has to be large enough to ensure no reset occurs during communication. Resets will be triggered if certain operating conditions are not fulfilled any more. Simple devices include voltage sensors that can suspend digital operations during communication and trigger a reset if the internal voltage level drops below a certain limit which is required to guarantee reliable operation. This can either be the case when digital or memory operations cannot be guaranteed any more – like writing or reading the electrically erasable programmable read only memory (EEPROM) – or analog functionality might be compromised – like bandgap voltages become instable. More complex devices can also incorporate sensors that survey operating temperature, exposure to intense light or rapid changes of the supply voltage [15].

C. Current consumption and required minimum H-field for chip operation

One of the main criteria for a contactless Smartcard transponder is its minimum operating field strength H_{MIN}, which defines the achievable operating distance with a reader, if power on the Smartcard is the limiting condition. Mainly two aspects take influence on H_{MIN}: Chip current consumption and the required antenna coil voltage for operation. For defined antenna and resonance conditions, the lower current consumption and coil voltage are, the lower will be the minimum required *H*-field for operation [18]. 3 operational phases can be critical regarding power consumption and have to be considered:

a) Communication of reader to card

In ISO/IEC14443A for reader data transmission at base data rate using amplitude shift keying (ASK) of 100 % modulation index, the contactless card power supply is turned off regularly (for 2 – 3 µs per bit duration of 9.44 µs at ~ 106 kbit/s). The reader command uses modified Miller coding as channel code [3]. During this off-keying of the carrier *H*-field, no power can be supplied to the card and internal operations must be supplied by the buffer capacitor. In most implementations, chip operations are suspended to a certain degree (e.g. data fetching blocks and security sensors stay active) during this communication phase, to save power and to be able to reduce buffer capacitor size to a minimum.

b) Power operations during full H- field present

The 2nd phase during which the supply voltage can drop concerns the time after a reader command was received, and some chip operation is required. A reset condition can occur, if internal operations draw more power than can be provided by the *H*-field. Digital or memory operations can draw peak currents and drain the buffer capacitor to a certain amount, but there is not much activity during the internal clock edges so that the capacitor can recharge again. However, if the overall current required exceeds the amount of current delivered by the field, the supply voltage will still drop.

c) Communication of card to reader

In the 3rd phase a situation similar to phase 1 occurs during the card modulation as here the coil pins are shorted in order to generate a load modulation which can be detected by the reader. Manchester coding of data on a 847.5 kHz subcarrier is used for channel coding [2]. The 847.5 kHz digital signal corresponds to much shorter state durations as PCD communication in phase 1. Thus also the time to recharge the internal buffer capacitor will be reduced and can result in a slowly dropping supply voltage if the required overall operating current exceeds the current provided by the *H*-field during the time of PICC modulation.

D. Load modulation

The PICC communication will be done by a load change that generates a subcarrier that can be detected by the PCD. The ISO14443-2 specifies the minimum level of the transponder load modulation depending on the operating *H*-field strength. Reader manufacturers must consider a similar limit for the sensitivity of the reader. In case the transponder LM is too low the reader probably can have difficulties to distinguish the transponder card communication from overlaid noise.

IV. COMMUNICATION SEQUENCE SIMULATION

When running system simulations certain criteria are essential for a well performing transponder front end.

It is of main interest to see the behavior of the transponder front end over process corner variations, operating field strength range and of resonance frequency variation. Our ISO model shown in fig. 5 allows to sweep the transponder resonance frequency by means of a tuning capacitor C_{TUNE} over a specified product range, reflecting tolerances of the chip and the inlay manufacturing process. A variation of the operating *H*-field strength can be determined by a variation of the voltage source U_D, representing the amplifier internal driver voltage. Process corner variations are simulated using appropriate process model files representing the spread of the chip manufacturing process for the transponder front end.

The test bench contains as stimulus a reference transaction covering all 3 operational phases as described in section III C.

A. Simulation of Resonance Frequency

For a proper investigation of various PICC parameters it is important to know at which operating frequency the simulation is run. Parameter influenced by the operating resonance frequency of the tag can be: H_{MIN}, *LM*, etc.

To check the plausibility of the simulation the following estimation can be used (15)

$$C_{TUNE} = \frac{1}{\omega_R^{\,2} L_{ANT}} - C_{ANT} - C_{CHIP} \qquad (15)$$

Where C_{ANT} is the parasitic transponder antenna capacitance, C_{CHIP} is the integrated capacitance for the specific operating condition, L_{ANT} is the transponder antenna inductance, and ω_R is the simulated radian resonance frequency, all nominal values.

To extract the right resonance frequency, the simulation method of an AC sweep can be performed and the current into the reader antenna is probed. To take into account the change of emitted *H*-field strength caused by the frequency variation in the amplifier voltage source, we calculate antenna current per *H*-field strength as a normalized parameter, instead of the current only. The frequency point where this parameter reaches its maximum defines the appropriate resonance frequency for the chosen tuning capacitor at this *H*-field.

All other simulations can then be run with the tuning capacitance values determined from these simulations.

B. Minimum operating field strength H_{MIN}

In order to determine the minimum operating field strength the circuitry has to be set to its operating resonance frequency like described above. Then a reference transaction using the simulation method of a transient simulation is performed. The reference transaction as described in section III C contains a specific PCD communication representing a worst case energy situation for the transponder (several consecutive symbols of Miller coded 0 or Miller coded 1). The PCD communication is followed by an internal operation with certain maximum power consumption (e.g. CPU operation, crypto operation, EEPROM read or write cycle). The 3rd part of the reference transaction contains a non-realistic PICC communication representing a worst case energy situation for the transponder (continuous 847.5 kHz modulation over a certain period of time). During the communication the voltage levels of the transponder chip need to be stable and are not allowed to drop below a certain reset value. If that happens the current provided by the field is not sufficient to perform the requested operation. If no reset occurs the *H*-field strength is strong enough to maintain the transponder operating.

Another important aspect to determine H_{MIN} is the communication ability of the device. Certainly a transponder can only be used properly if all phases of communication are possible. Thus the transponder chip demodulator shall be capable of detecting a PCD communication even below H_{MIN}. A reason therefore is that often there are operations which consume less power than the reference transaction and those can still be performed even when less *H*-field strength is available. In order to verify this, the demodulator signal has to be probed during simulations.

C. Reader command demodulation for ISO/IEC14443A base data rate

The communication air interface specifications in ISO/IEC14443-2A allow a variety of different *H*-field amplitude envelopes for channel coding of the PCD communication, using modified Miller code, which the transponder chip demodulator must be capable of handling. To ensure the demodulator can handle all the allowed communication signals accordingly, various envelope shapes on 13.56 MHz carrier can be applied as stimulus at the amplifier voltage source into the ISO model and be simulated over different *H*-field strength, temperature, process corners and resonance frequencies. To verify the functionality in the lab, the same amplitude envelope shapes can be measured there as well.

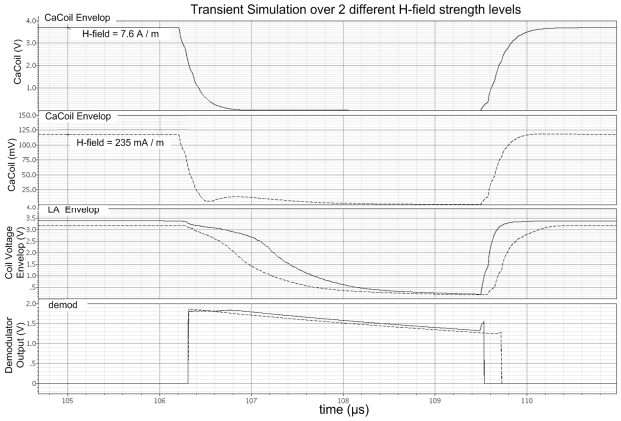

Figure 8. Calibration coil voltage, transponder coil voltage and demodulator output voltage during PCD communication at 2 different *H*-field strengths.

The main challenge in the concept of the whole transponder front end is to provide enough sensitivity for the demodulator to function properly over a wide range of various input parameters (like temperature e.g. – 40 °C - + 100 °C, *H*-field e.g. 1.5 – 7.5 A/m, supply voltage e.g. 1.2 – 1.9 V_{DC} and process corners e.g. slow and fast CMOS transistor transition times). Due to the operating conditions of the front end the signal shape seen on the coil pins can be severely different to what can be observed with the Calibration Coil at the air interface. An example is given in fig. 8.

D. Load modulation

To simulate the LM a periodic steady-state (PSS) analysis can be used. This parameter considers the impact of the transponder modulation on the Reader antenna circuit. The ISO/IEC10373-6 antenna arrangement specifies two equal sense coils in equal distance to the emitting PCD loop antenna, which provide a spatial filtering, for this purpose. Connected as a zero-compensation bridge, this so-called "Helmholtz-arrangement" allows to compensate the induced voltage of the primary *H*-field of the PCD antenna and so to measure in good quality the secondary *H*-field of the transponder, which contains the load modulation signal.

The Helmholtz bridge output V_{HELMH} of the model is probed and the levels of load modulation at 13.56 MHz ± 847.5 kHz are measured in frequency domain. The Proximity base standard [2] specifies a minimum limit V_{LMLIM} of $V_{LM} = 22/\sqrt{H_{RMS}}$ in a range of H_{MIN} to H_{MAX} (e.g. 1.5A/m to 7.5A/m for class 1 antenna size) for a transponder card. Depending on the implementation on chip the actually measured value V_{LM} might change over *H*-field strength or stay relatively constant. This depends how much the voltage used for generating the modulation varies over field strength and how the modulation transistor gate is controlled. The plot below shows the LM levels of the presented Proximity transponder front-end.

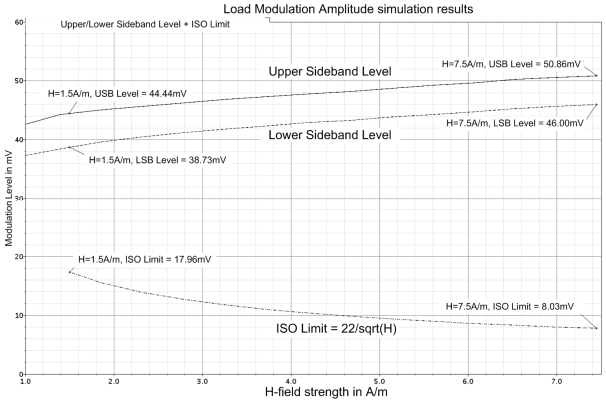

Figure 9. Upper and lower load modulation sideband levels in comparison with minimum limit specified in ISO/IEC14443-2.

V. Conclusion

The presented ISO/IEC14443 compliant transponder chip has been manufactured in a 140 nm CMOS process and was measured in the laboratory. For the measurements an automated test setup was used, capable of sweeping the *H*-field strength over the specified range at specific defined temperature levels. A class1 antenna was used that had to be adjusted to a number of defined resonance frequencies by means of a tuning capacitor. The results of the measurements were compared to simulation results using the described ISO model and performing the simulations in a way like described in section IV. The comparison shows pretty good matching for simulation and measurement data, confirming the reliability of the model, the data obtained from the class1 antenna used for the measurements and the transponder front end designed in a 140 nm CMOS process. As there is a high demand to mount contactless transponders into various different shaped devices antenna classes smaller than class 1 are becoming more and more important. The draft standard defines them in [6-8] and the developed ISO model can be used to compare transponder measurements and simulation results for the antenna classes 2-6 as well.

REFERENCES

[1] ISO/IEC14443-1: *Identification cards – Contactless integrated circuit cards – Proximity cards – Part 1: Physical characteristics*, second edition, June 2008.

[2] ISO/IEC14443-2: *Identification cards – Contactless integrated circuit cards – Proximity cards – Part 2: Radio frequency power and signal interface*, second edition, Sept. 2010.

[3] ISO/IEC14443-3: *Identification cards – Contactless integrated circuit cards – Proximity cards – Part 3: Initialization and anticollision*, second edition, Nov. 2009.

[4] ISO/IEC14443-4: *Identification cards – Contactless integrated circuit cards – Proximity cards – Part 4: Transmission protocol*, second edition, July 2008.

[5] ISO/IEC10373-6: *Identification cards – Test methods – Part 6: Proximity cards*, second edition, Jan. 2011.

[6] ISO/IEC JTC1 SC17 N3994: *ISO/IEC 14443-1:2008/AM1: Additional PICC Classes, April 2010.*

[7] ISO/IEC JTC1 SC17 WG8 N1738: *ISO/IEC 14443-2:2008/FPDAM4.3: Additional PICC Classes, Sept. 2010*

[8] ISO/IEC JTC1 SC17 WG8 N1740, *ISO/IEC10373-6: FPDAM 8.3, Additional PICC Classes*, Oct. 2010.

[9] C. Weidinger, "An FPGA verification flow for RFID smart label transponder ICs (13.56 MHz), Austrochip 2003.

[10] A. Vena, P. Roux, "Near field coupling with small RFID objects", Proc. of Progress in electromagnetics research Symposium, pp. 535 – 539, Aug. 2009.

[11] W. Lin, B. Geck, H. Eul, C. Lanschützer, P. Raggam, "A novel method for determining the resonance frequency of PICCs", CSNDSP, pp. 311 – 315, 2008.

[12] L. Dong-sheng, Z. Xue-sheng, Y. Qiu-ping, X. Ting-wen, "An alalogue front-end circuit for ISO/IEC15693-compatible RFIC transponder IC", Journal of Zhejiang University Science A, pp. 1765 – 1771, July 2006.

[13] Z. Zhou, B. Jamali, P. H. Cole, "Brief comparison of different rectifier structures for HF and UHF RFID (Phase I/II)", Auto-ID Labs, 2004.

[14] H. Plötz, "Mifare Classic – Eine Analyse der Implementierung", Diplomarbeit am Institut für Informatik der Humboldt-Universität zu Berlin, 18. 8. 2008.

[15] H. Li, "Security evaluation at design time for cryptographic hardware", Technical report no 665, Computer Lab, Univ. of Cambridge, ISSN 1476-2986, April 2006.

[16] M. Gebhart, S. Birnstingl, J. Bruckbauer, E. Merlin, "Properties of a test bench to verify Standard Compliance of Proximity Transponders", in CSNDSP, July 2008, pp. 306-310.

[17] M. Gebhart, B. Flecker, *Lecture notes on RFID Systems*, course 440.417, Dept. of Communication Networks and Satellite Communications, Graz University of Technology, http://www.iks.tugraz.at/lehre/unterlagen/rfid-systems/.

[18] M. Gebhart, M. Wienand, J. Bruckbauer, S. Birnstingl, "Automatic Analysis of 13.56 MHz Reader Command modulation pulses", Eurasip RFID Workshop 2008.

[19] M. Gebhart, "Analytical considerations for an ISO/IEC14443 compliant Smartcard", to be published in ConTEL 2011